A Multiphase Approach to Model Blood Flow in Micro-tubes

T. M. Mubita, L. R. Rojas-Solórzano and J. B. Moreno

Abstract The development of micro-fluidic devices to support the systemic circulation of blood has been used either as a temporary bridge or as a recovery method to treat different heart diseases. Blood flow through these artificial micro-channels is a major challenge because blood at scales from tens to hundreds of microns behaves as a multiphase suspension of deformable particles. A homogeneous model of blood is not adequate if the effect of cell segregation through these devices is of interest to evaluate blood cell damage (e.g., hemolysis or thrombosis). To determine the flow field and model the occurrence of segregation, an Eulerian frame of reference is employed. The simulations are performed in a tube of internal diameter of $217\,\mu\text{m}$. We find that the results contribute to improve the understanding of the fluid dynamics of blood as a multi-component medium. Our simulations are based on an alternative methodology for blood modelling at a lower computational cost compared to DNS.

1 Introduction

The use of micro-fluidic components has become important in developing equipment for blood transport. During the design process, it is critical to predict the location of regions with large damage generation and potential deposition of blood aggregates in order to minimize these conditions. This fact is particularly relevant to devices

T. M. Mubita · J. B. Moreno
Department of Thermodynamics and Transport Phenomena, Universidad Simón Bolívar, USB, Apartado Postal 89000, Caracas, Venezuela
e-mail: 08-86884@usb.ve

J. B. Moreno
e-mail: morenoj@usb.ve

L. R. Rojas-Solórzano (✉)
School of Engineering, Nazarbayev University, Astana 010000, Republic of Kazakhstan
e-mail: luis.rojas@nu.edu.kz

containing small channels, junctions, or gaps, in which near wall shear forces and contact with a foreign surface can cause cell activation or damage.

To accurately predict the rate of damage in these "hot spot" zones, it is very important to take into account that blood can be regarded as a homogeneous fluid at a macroscopic level, while at the microscopic level, blood must be considered as a tissue comprising various types of cells (i.e., red blood cells, RBCs; white blood cells, WBCs; and platelets, PLTs) and a liquid intercellular material (i.e., the plasma). This corpuscular nature of blood makes the blood cells have different flow patterns under microcirculation, which are distributed in different regions around the conduct where they flow through.

It has been well recognized that in the flow of blood, the mutual interactions of the RBCs with each other and with platelets lead to an organization of these individual blood components, such that RBCs tend to accumulate at the centreline of the blood vessels (the Fahraeus–Lindquist effect), while platelets are observed to be displaced laterally towards the walls of the vessels in a non-diffusive manner (Almomani et al. 2008).

It has also been reported that due to the presence of RBCs, an increased platelet concentration near the wall (platelet margination) can be observed. In dilute-rich plasma, suspension platelets behave similarly to rigid particles and accumulate at a radial location near 60 % of the tube radius (Aarts et al. 1988). Goldsmith et al. (1995) studied whether red cells exert a physical or chemical effect that promotes aggregation of platelets. Zhao et al. (2008) studied a suspension of RBCs and platelet-sized fluorescent polystyrene particles at controlled flow rates (6–$30\,\mathrm{mL\,h^{-1}}$) through a micro-channel containing a 100–$200\,\mu\mathrm{m}$ expansion. Zhao et al.'s work focused on determining the effect of hematocrit on the enhanced platelet concentration in sudden expansions.

Numerical simulations and mathematical formulations have been conducted by a number of research groups to model the spatial distributions of blood elements. Approaches like kinetic theory model, employed by Gidaspow and Huang (2009) and mixture theory model proposed by Massoudi and Antaki (2008) only assume blood as a mixture consisting of RBCs suspended in the plasma, while ignoring the presence of other cells. A two-blood-cell approach was used by Yeh et al. (1994), who characterized the platelet lateral migration (i.e., towards the wall) using a convective diffusive transport equation for platelets, and incorporating an empirical drift function, based on the flow visualization of RBCs and platelet-sized latex beads solutions in a micro-tube. Jung and Hassanein (2008) used the averaging technique to simulate leukocyte migration due to flow-dependent interactions with RBCs within disturbed flow in a sudden expansion and a carotid artery by using a multiphase non-Newtonian model. Jung and Hassanein's research constitutes a good approach in which the multiphase nature of the blood is taken into account despite there is not enough information about how they validated the model.

The aim of this research is to propose and validate a numerical model of blood flow that uses a multiphase computational fluid dynamics approach, to investigate the blood flow behaviour at the microscopic level in order to gain accurate insight into the detailed migration of blood cells within a straight micro-tube.
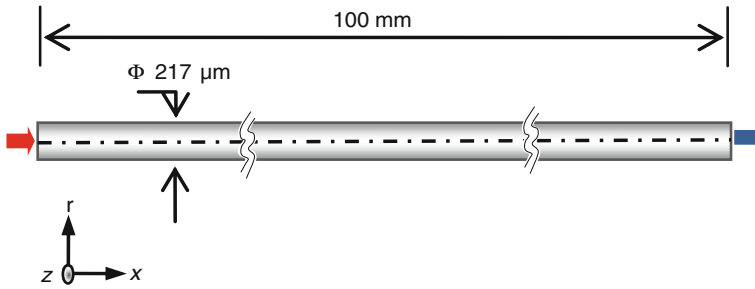
Fig. 1 Computational domain

2 Physical Properties and Numerical Set-up

2.1 Computational Domain and Boundary Conditions

The numerical simulations are performed using an Eulerian–Eulerian multiphase model. The blood is considered as a fluid that consists of plasma, RBCs, and PLTs. The plasma is modelled as a continuous Newtonian fluid with a viscosity of 0.0012 Pa-s and a density of 1,025 kg m^{-3}. RBCs and PLTs are taken as a spherical particle-like fluid dispersed with a density of 1,100 and 1,040 kg m^{-3}, respectively. Sauter mean diameters of 6 µm for RBCs and 2.5 µm for PLTs are assumed. In this study, the viscosity of the disperse phases is considered to be constant through the computational domain, with a value of 0.002 Pa s.

Figure 1 illustrates a schematic of the computational domain showing the tube with a constant cross-section. The internal diameter of the tube is 217 µm (equivalent to ~35 times the mean Sauter diameter of RBCs) and the geometry is depicted by assuming axis-symmetry. At the beginning of the simulation, the whole tube was full of a uniform mixture of plasma, RBCs, and PLTs with volume fractions (α) of 58, 40, and 2 %, respectively. The inlet flow is adjusted such that the axial velocities within the tube lead to similar values to the equivalent Poiseuille average wall shear rate of 555 s^{-1} used by Yeh et al. (1994). Initially, the radial velocities of each phase were set to zero. A free-stress boundary condition is assumed at the exit of the domain, while a zero velocity/no-slip condition is assumed at the walls. Because of the low Reynolds number (<5), turbulence effects were not considered.

2.2 Computational Methodology

The numerical simulations of the 3D, steady, laminar, multiphase flow are performed using ANSYS-CFX ® v12. The numerical model proposed is based on the Eulerian-Eulerian approach. The conservation equations for multiphase flows are presented below. The continuity equation for each phase (k = plasma, RBCs, or PLTs) is given

by:

$$\frac{\partial \alpha_k \rho_k}{\partial t} + \nabla.(\alpha_k \rho_k \mathbf{u}_k) = 0 \tag{1}$$

where t is time, ρ_k, α_k, and u_k are, respectively, the density, volume fraction, and velocity vector of phase k. In addition, the volume fraction of each phase must satisfy the following constraint,

$$\sum_{k=1}^{n} \alpha_k = 1, \tag{2}$$

with $n = 3$ being the total number of phases. The volume fraction occupied by one phase cannot be occupied by other phases.

The momentum equation for each phase is given:

$$\frac{\partial}{\partial t}(\alpha_k \rho_k \mathbf{u}_k) + \nabla.(\alpha_k \rho_k \mathbf{u}_k \mathbf{u}_k)$$
$$= -\alpha_k \nabla_p + \nabla \cdot \tau_k + \alpha_k \rho_k \mathbf{g}$$
$$+ \sum_{P=1}^{n} R_{kl}(\mathbf{u}_k - \mathbf{u}_1) + \mathbf{F}, \tag{3}$$

where p is the pressure shared by all phases, $\mathbf{g}$ is the gravity, $R_k l$ is the interaction force coefficient between the continuum and disperse phases, which depends on the geometry of the interface and local slip Reynolds number, $\mathbf{F}$ is a force term containing the lift force, virtual mass, and drag, and τ_k is the stress tensor of phase k for Newtonian fluids, given by:

$$\tau_k = \alpha_k \mu_k (\nabla \mathbf{u}_k + \nabla \mathbf{u}_k^T) + \alpha_k \left(\lambda_k - \frac{2}{3} \mu_k \right) (\nabla \cdot \mathbf{u}_k)\mathbf{I}, \tag{4}$$

where μ_k and λ_k are, respectively, the dynamic and bulk viscosity of phase k, and $\mathbf{I}$ is the unit tensor.

2.3 Verification of Grid Independence

A second-order discretization scheme is used to calculate the advection terms in the discrete finite volume equations. The standard calculation is case-dependent and takes a CPU time from 8 to 36 h on a processor AMD Turion64 with operative systems MS Windows 7, SP2.

In order to corroborate that the solution is independent of the grid resolution, a study of grid convergence is undertaken. With this study, the truncation error is reduced and the best degree of grid resolution is defined. The method consists of iterative and parameter convergence studies using multiple solutions with sys-

Table 1 Uniform structured grids with total number of cells

Mesh	Elements
Coarse	61,740
Medium	152,920
Fine	387,266

tematic parameter refinement to estimate numerical errors and uncertainties. The adopted method for discretization error estimation is the Grid Convergence Index (GCI) based on the Richardson Extrapolation (RE) method, which involves comparisons between three different grid sizes (Roache 1994). The GCI method has shown good performance for numerous and different CFD applications. In order to quantify the discretization error, the systematic procedure recommended by Celik (2008) is followed. The method considers the situation for three solutions corresponding to fine ϕ_1, medium ϕ_2, and coarse ϕ_3 grids with hexahedral elements; three convergence conditions are possible: (i) monotonic convergence; (ii) oscillatory convergence; and (iii) divergence.

The finite element meshes carefully modelled the near-wall region. Table 1, gives the number of computational cells for each one of the meshes generated. The refinement factors, $r_{21} = h_{medium}/h_{fine}$ and $r_{32} = h_{coarse}/h_{medium}$, which are based on a representative cell, mesh, or grid size h, were 1.3 in all cases. The grid refinement should be done systematically; the use of a constant parameter refinement ratio is not required but simplifies the analysis. Celik (2008) suggested that a factor greater than 1.3 would be desirable, based on experience and not on formal derivation. As illustrated in Fig. 2a, there is a reduction of the PLTs volume fraction as the grid is refined, indicating that the dependence of the numerical simulation on the cell size is reduced. Further refinement of the grid will give oscillatory convergence in most of the measurements points, which is an indication of the small difference between the results of the grids.

The three grids used with the GCI method showed that the apparent order of accuracy ranges from 2.64 to 13.96, with an average of 7.15 in the measurement line located at 70 mm from the inlet. This averaged apparent order of accuracy is used to assess the GCI index values for individual grids, which is plotted in the form of error bars, as shown in Fig. 2b. The maximum discretization uncertainty is 6.52 % with an average value of 1.39 %; the highest differences obtained occur at distances from 5.9 to 6.8 μm from the tube wall.

3 Results and Discussions

The blood cells are modelled as liquid dispersed droplets in a three-dimensional Poiseuille flow with gravitational acceleration perpendicular to the tube axis, where the Froude number is 0.33. The section of the micro-tube subjected to analysis corresponds to a region of hydrodynamically developed flow far downstream from the inlet.

Fig. 2 a Platelets
concentration profile in a
section of the tube obtained
for three different meshes,
b Medium-grid solution, with
discretization error bars
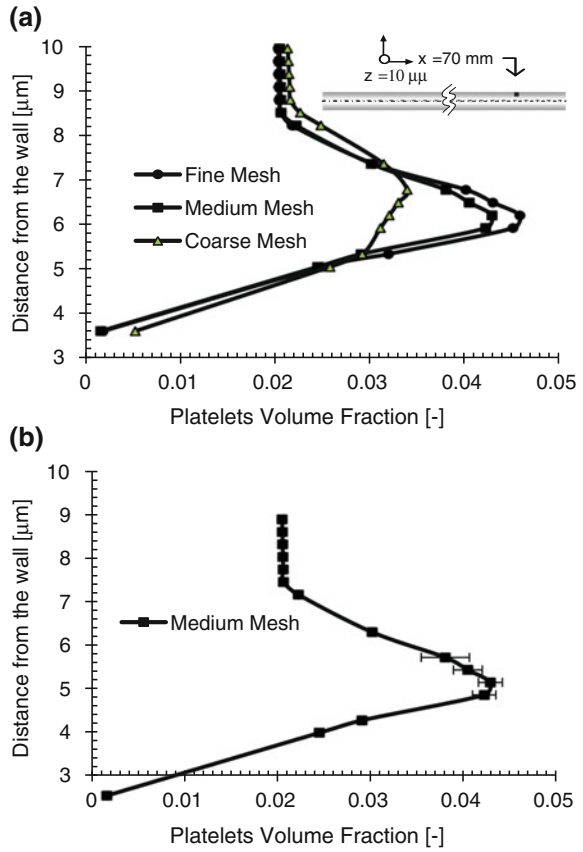
Fig. 3 Platelets' volume
fraction. The Reynolds
number as calculated at the
inlet of the channel was
$Re_{PLTs} = 1.62$

(a)

(b)
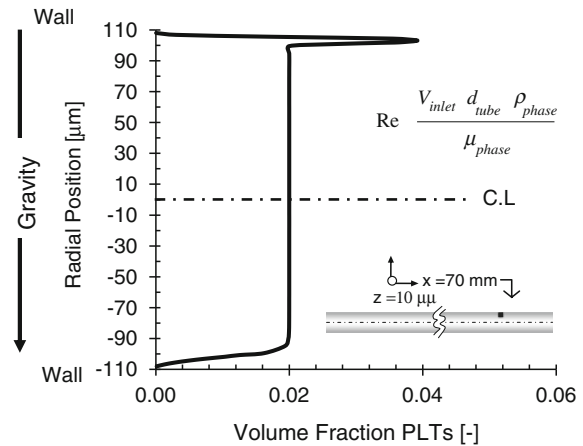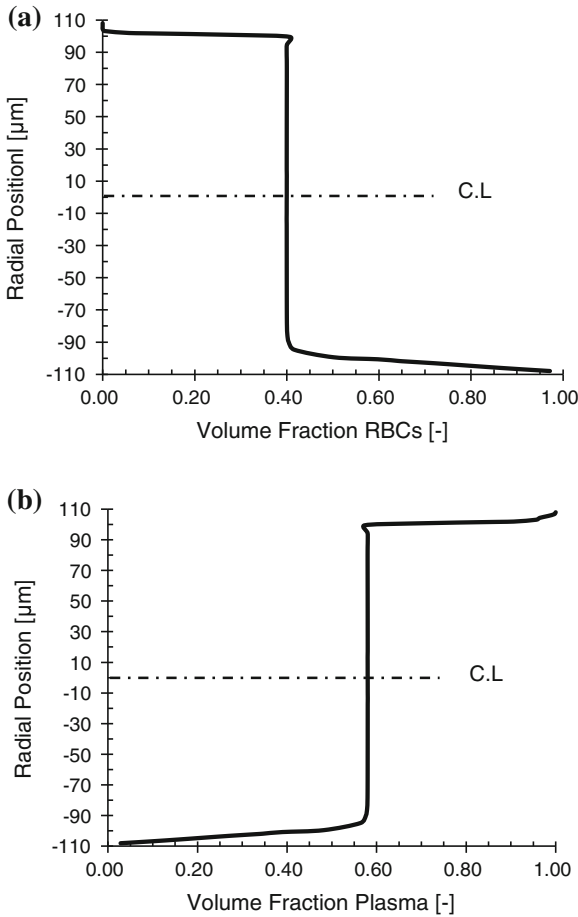
Fig. 4 **a** RBCs concentration profile, Reynolds number, calculated at the inlet of the channel, $Re_{RBCs} = 1.71$, **b** Plasma concentration profile, $Re_{Plasma} = 2.62$

The volume fraction of the disperse phases and plasma are plotted as a function of the radial location in Figs. 3 and 4.

Because of the low Froude number, RBCs tend to migrate towards the bottom of the pipe, increasing their concentration in this region. As they are settled down, a displacement of plasma and platelets occurs towards the upper side of the pipe. The maximum concentration of plasma and RBCs are in the upper and bottom wall, respectively. However, in the case of PLTs, the highest concentration is located very near the upper wall. This behaviour has been reported by several authors for neutrally buoyant solid spherical particles (Won and Yul 2008), buoyant particles (Hogg 1994), drops (Nourbakhsh and Mortazavi 2010), and in Eckstein et al. (1988)'s work, where they found that this behaviour is also characteristic of the flow of platelets

Fig. 5 Comparison between the platelets' concentration profile as obtained experimentally and numerically. The error bars represent the relative errors of computed results
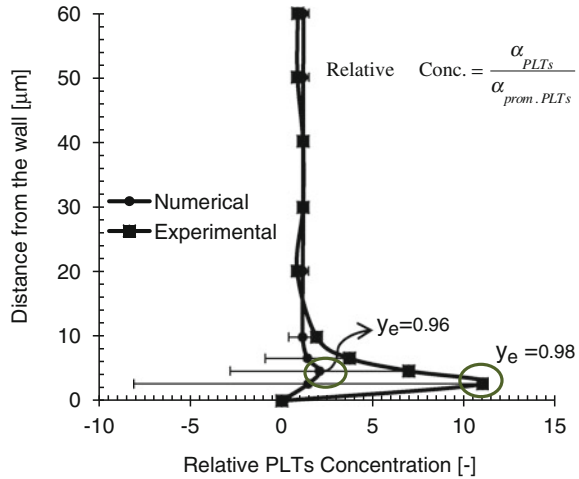

in microcirculation. In general, this behaviour is related to multiphase flow, when the relationship between the channel size and the particle size is relatively large and the Reynolds number (Re) is low.

The peak in the platelets concentration profile is attributed to a lateral migration of particles that tend to cluster at a distance from the wall known as the *equilibrium position* y_e, which is defined as the lateral distance from the centreline of the channel to the peak position of the particle concentration distribution, (r/R). According to Ho and Leal (1974) and the first studies of Segré and Silberberg (1962), using spherical particles with neutral buoyancy, it is observed that in the absence of any slip velocity, the particles tend to migrate away from the wall and the centreline canals, accumulating in an equilibrium position equal to 0.6. However, if we compare with the results reported by Yeh et al. (1994) for a geometry equal to the one used in this chapter (see Fig. 5), the equilibrium position for their experimental data is 0.98, while in our simulation is 0.96, yielding approximately a relative error of 2 %. In addition, we may see that our model is able to predict the platelet concentration at the centre of the pipe; though as we approach to the wall, the concentration numerically obtained is approximately five times lower than that reported experimentally.

To analyze the reason for this deviation, it is important to note that Tilles and Eckstein (1987), Aarts et al. (1988), and Zhao et al. (2007) among others, have reported that the margination and accumulation of platelets in a region near the wall is influenced mainly by the hydrodynamic interaction of these cells with the red blood ones, thus increasing its concentration as the hematocrit increases. In principle, the deviation can be explained by the fact that our computational model does not take into account the interactions among the disperse phases, but only those between the disperse and continuum phases, under the assumption that each phase is present in each control volume and has a volume fraction equal to the fraction of the control volume occupied by that phase.

Fig. 6 Radial profiles of the forces that affect the movement of the phases through the tube
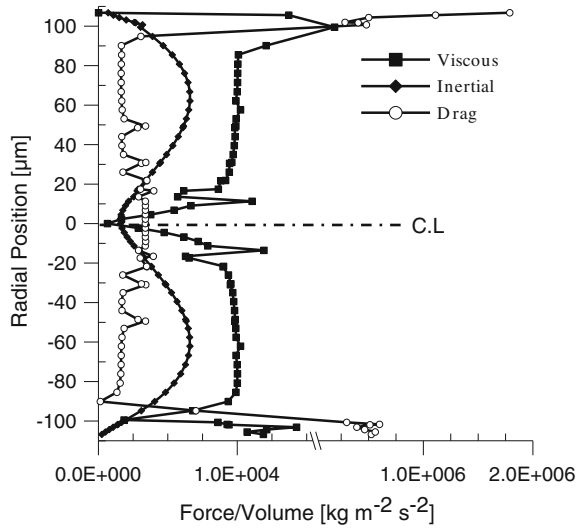
Since in this case the Froude number is very small, PLTs lateral migration is controlled by gravity. RBCs, which are heavier than the fluid, migrated to the bottom of the tube, while all PLTs eventually tended to migrate to the top. Therefore, in a given section of the pipe there is a single equilibrium position. A region of dense solids can be supported by a less concentrated (and therefore, less-dense) layer owing to the interplay of sedimentation and shear-induced diffusion (Matas et al. 2004).

In addition, the interplay of viscous, drag, and inertial forces gives rise to a variety of possible fluid phase distributions. Ranking the importance of different forces helps predicting multiphase flow behaviour. In Fig. 6, the different forces are plotted in the radial position. The drag force, due primarily to the viscous nature of the carrier-continuum fluid phase, is dominant at the walls and is responsible for entraining particles along the flow main stream. The lateral dispersion, responsible for the transverse migration of particles across the flow streamlines, is likely to be dominated by the wall inertial forces.

It is clear that the drag force increases as the distance between the wall and the particles decreases. The increase is due to viscous effects derived from the wall presence; when the particle Reynolds number, $Re_p = d_p u_s / \nu$, is small, the inertial term in the Navier-Stokes equations is small compared to the viscous term at distances of the order of the particle radius, $d_p/2$, from the particle centre. Here u_s is the dimensional magnitude of the slip velocity and ν is the kinematic viscosity of the continuous phase.

The buoyant weight of the particles defines a slip velocity that can be either upward or downward, depending of the disperse phase concentration ratio (see Fig. 7). Although, in our case the difference is not so remarkable, this small variation is the effect of the particle migration close to the tube wall which generates a wall-induced lift force, driving the PLTs away from the wall.

T. M. Mubita et al.

Fig. 7 Platelets slip velocity obtained by varying the volume fraction of phases
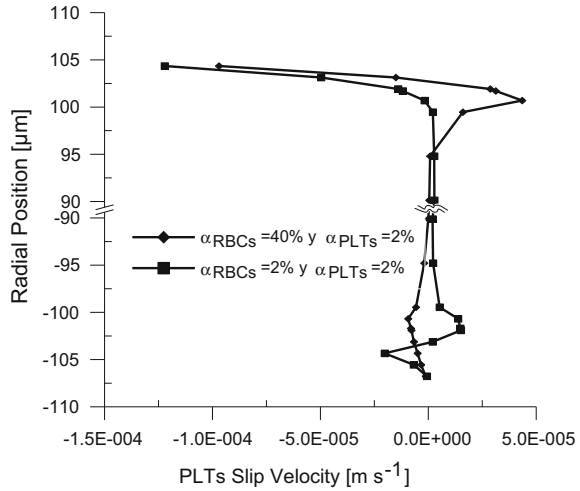
It is important to note that the lateral migration is only observed in the PLTs, while for RBCs only sedimentation occurs. This implies that the phenomenon depends on the size of the particles among other factors. This can be seen in Fig. 8, where the results are compared when PLTs and RBCs are modelled by assuming they have the same volume fraction (2 %) or when they have volume fractions of 2 and 40 %, respectively.

The peak of highest concentration is still observed for the platelet phase at the same equilibrium position. However, it is placed to the other side of the tube. For RBCs, the concentration profile does not change even though the volume fraction varies from 40 to 2 %.

Since the density difference between the plasma and the platelets is small and the platelet diameters are smaller than the RBC ones, the magnitude of the gravitational force is higher for RBCs and makes the major contribution to the motion of these particles. So, if the particle is only slightly buoyant, it stabilizes at a position close to the wall, and depending on the concentration of the other disperse phases, this will be at the top or at the bottom of the tube. In this case, the particles have sufficient buoyancy to dominate the far field of the velocity field, but insufficient to affect the region where there is a balance of the viscous forces with the shear advection term. Then, platelets cannot go all the way onto the wall because of the repulsion and so it will stabilize at a stand-off distance from one of the walls.

For larger buoyancy, the migration of the phase settling under gravity resembles that caused by a sedimenting particle, and therefore the effect of shear and wall repulsion is negligible.

Fig. 8 Concentration profile when varying the volume fraction of the dispersed phase at the tube inlet: **a** platelets, **b** red blood cells
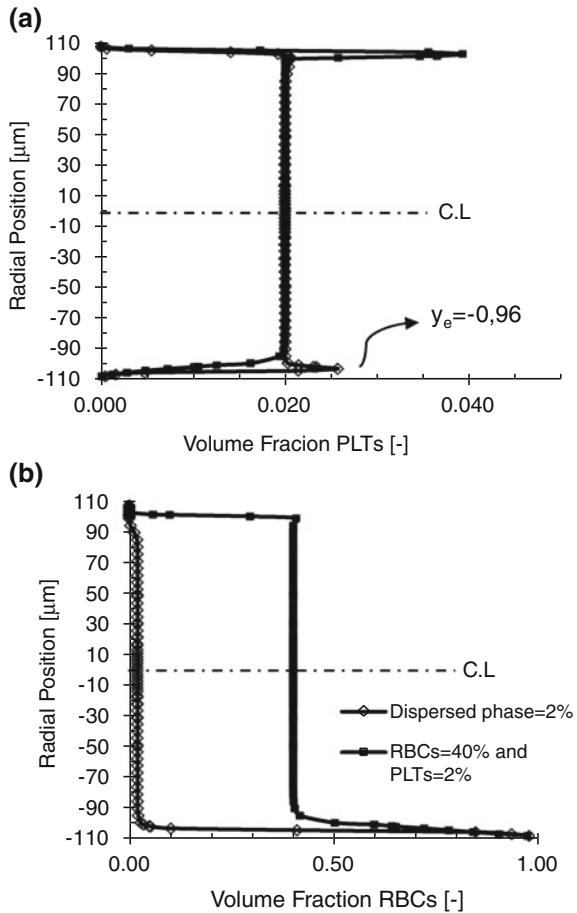
4 Concluding Remarks

Numerical simulations of the motion of two disperse phases, of different densities and concentrations, have been carried out in order to model the migration of blood cells through a micro-tube.

In summary, although the physical mechanisms of the lateral migration are complex and are still under active research, we have presented a simple and accurate approach to model the movement of blood cells through micro-conducts. The results obtained in this investigation show that the underlying dynamics is due to the competition of three effects: one linked to wall-induced shear stress, producing a core-ward drift; one associated to the shear and the curvature of the Poiseuille flow, producing a motion towards the wall (Ho and Leal 1974); and the other one related to the

concentration and diameter of the disperse phases, which become a key factor when the phases are not neutrally buoyant.

It should be pointed out that although the scenario of platelet cell migration in microcirculation is qualitatively described by our numerical simulation, we were unable to quantitatively account for the effects of the RBCs migration. In this sense, we may state that the numerical model is able to describe with a good approximation the physical phenomenon of segregation, but further fine tune-up is still required to account for the effects of RBCs migration on the PLTs segregation.

References

Aarts P, van den Broek S, Prins G, Kuiken G, Sixma J, Heethaar R (1988) Blood platelets are concentrated near the wall and red blood cells, in the center in flowing blood. Arterioscler Thromb Vasc Biol 8:819–824

Almomani T, Udaykumar H, Marshall J, Chandran K (2008) Micro-scale dynamic simulation of erythrocyte-platelet interaction in blood flow. Ann Biomed Eng 36:905–920

Celik I (2008) Procedure for estimation and reporting of discretization error in CFD applications. J Fluid Eng 130:1–4

Eckstein E, Tilles A (1988) Conditions for the ocurrence of large near wall excess of small particles during blood flow. Microvasc Res 36:31–39

Gidaspow D, Huang J (2009) Kinetic theory based model for blood flow and its viscosity. Ann Biomed Eng 37:1534–1545

Goldsmith H, Bell D, Braovac S, Steinberg A, McIntosh F (1995) Physical and chemical effects of red cells in the shear-induced aggregation of human platelets. Biophys J 69:1584–1595

Ho B, Leal L (1974) Inertial migration of rigid spheres in two-dimensional unidirectional flows. J Fluid Mech 65:365–400

Hogg A (1994) The inertial migration of non-neutrally buoyant spherical particles in two-dimensional shera flows. J Fluid Mech 272:285–318

Jung J, Hassanein A (2008) Three-phase CFD analytical modeling of blood flow. Med Eng Phys 30:91–103

Massoudi M, Antaki J (2008) An anisotropic constitutive equation for the stress tensor of blood based on mixture theory. Math Prob Eng 2008:1–30

Matas J, Morris J, Guazzelli E (2004) Lateral forces on a sphere. Oil Gas Sci Technol Rev IFP 50:59–70

Nourbakhsh A, Mortazavi S (2010) A three dimensional study of the motion of a drop in plane Poiseuille flow at finite Reynolds numbers. Iranian J Sci Technol Trans B Eng 34:179–196

Roache P (1994) Perspective: a method for uniform reporting of grid refinement studies. J Fluid Eng 116:405–413

Segré G, Silberberg A (1962) Behaviour of macroscopic rigid spheres in Poiseuille flow: part 2. Experimental results and interpretation. J Fluid Mech 14:136–157

Tilles A, Eckstein E (1987) The near wall excess of platelets-sized particles in blood flow: Its dependance on hematocrit and wall shear rate. Microvasc. Res. 33:211–223

Won Y, Yul J (2008) The lateral migration of neutrally-buoyant spheres transported through square microchannels. J Micromech Microeng 18:065015

Yeh C, Calvez A, Eckstein E (1994) An estimated shape function for drift in a platelet-transport model. Biophys J 67:1252–1259

Zhao R, Kameneva M, Antaki J (2007) Investigation of platelet margination phenomena at elevated shear stress. Biorheology 44:161–177

Zhao R, Marhefka J, Shu F, Hund S, Kameneva M, Antaki J (2008) Micro-Flow visualization of red blood cell-enhanced platelet concentration at sudden expansion. Ann Biomed Eng 36:1130–1141